Sonochemistry: A Greener Protocol for Nanoparticles Synthesis

6

Aniruddha B. Patil and Bhalchandra M. Bhanage

Contents

Abstract

Current nanoparticles synthetic methodologies are focused on greener aspects which eliminate or minimize the use of hazardous chemicals or conventional energy sources. Typical greener techniques involve the use of sonochemical, microwave, electrochemical, hydrothermal, supercritical solvents, biosynthesis, and solar energy. Among this sonochemical route of nanoparticles synthesis is a well-developed and well-explored area due to its simplicity and diverse applicability. Sonochemistry arises from acoustic cavitation which involves the formation, growth, and implosive collapse of bubbles in a liquid which create high pressure and temperature followed by high rate of cooling. These properties are often responsible for shape and size selective nanoparticles synthesis.

A.B. Patil • B.M. Bhanage (✉)
Department of Chemistry, Institute of Chemical Technology, Matunga, Mumbai, India
e-mail: bm.bhanage@ictmumbai.edu.in; bm.bhanage@gmail.com

M. Aliofkhazraei (ed.), *Handbook of Nanoparticles*,
DOI 10.1007/978-3-319-15338-4_4

Present chapter mainly focused on the basic concept of ultrasound and its application toward the synthesis of inorganic nanocrystalline materials like nanoparticles of metal, metal oxides, and metal sulfides. In addition, it covers the USP system for nanosize material synthesis.

Introduction

The area of nanoscience and nanotechnology is a center of current research activities that is growing with an enormous rate. The property of nanomaterials depends on the characteristics such as size distribution, grain size, grain boundaries, presence of free surface, heterophase interfaces, chemical composition of the constituent phases, and interactions among the constituent domains. These characteristics regulate the properties of nanomaterials, which are quite diverse from that of the bulk materials. Nanomaterials bridge the gap between the solid state and the molecular level that revels unique physicochemical properties showing novel technological applications. The area of nanostructured materials has opened up with new prospect in electronics, catalysis, energy, materials chemistry, and even biology [1] (Table 1).

The properties and applications of nanostructured materials are mainly associated with preparation method, and hence the appropriate selection of synthesis route ultimately determines the performance of nanostructured materials. Definitely, this has escort scientists' attention to the development of versatile synthesis techniques for the preparation of diverse nanomaterials. The synthetic protocols applied for nanoparticle preparation, including gas phase method (e.g., laser pyrolysis

Table 1 Available green methods for nanomaterial synthesis

Method of synthesis	Nanomaterial	Shape of nanomaterial	Size of nanomaterial	References
Sonochemical	Molybdenum carbide	Face centered cubic (fcc)	2 nm	[2]
Microwave	Zinc oxide	Polygonal	40 nm	[3]
	Zinc oxide	Triangular	20 nm	[4]
	$Mg(OH)_2$ and MgO	$Mg(OH)_2$ one-dimensional rod-like spherical	77 nm 45 nm	[5]
	Cuprous oxide	Spherical	38 nm	[6]
Electrochemical	Pd (0) nanoparticles	Spherical	5.91 ± 1 nm	[7]
Solar energy	Pd (0) nanoparticles	Multiple twinned particles	30–45 nm	[8]
	ZnO	Triangular and hexagonal	10–15 nm	[9]
	Pd (0) nanoparticles	Decahedral	30–45 nm	[10]

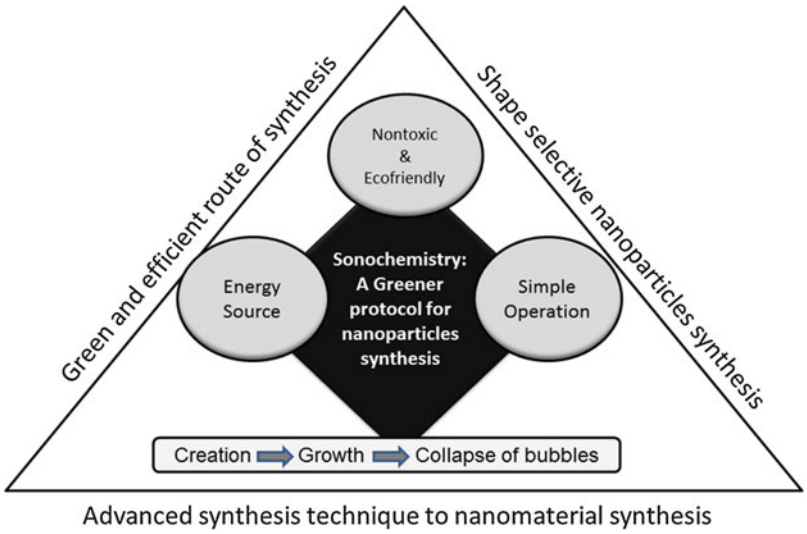

Fig. 1 Schematic representation of sonochemistry as a green energy source for nanomaterial synthesis

decomposition of volatile organometallics and molten metal evaporation), liquid phase methods (e.g., metal precursor reduction using diverse reductants), as well as mixed phase approaches (e.g., deposition of metal atom vapor into cryogenic fluids and synthesis of conventional heterogeneous catalysts on oxide supports). The above-stated protocol often entails the harsh reaction conditions like application of organic surfactants/solvents and strong reducing agents that results into generation of hazardous waste. In addition, the conventional nanoparticles synthesis methods found to be expensive. Hence, green and cost-effective alternative approach becomes more desirable for the preparation of nanomaterial that bypasses hazardous reagents. A typical greener technique involves the use of conventional energy sources like the use of sonochemical [2], microwaves [3–6], electrochemical [7], hydrothermal methods eliminating toxic reagents, supercritical CO_2, biosynthesis, and solar energy [8–10].

In consideration to abovementioned conventional and nonconventional techniques, the ultrasound application for nanomaterial's preparation has a well-developed and well-explored area; that is because of its simplicity and diverse applicability. The basic idea of sonochemistry arises from acoustic cavitation, which includes the formation of bubbles followed by growth, and implosive collapse that results high pressure as well as temperature followed by high cooling rate (Fig. 1).

So far the variety of inorganic nanoparticles was reported by sonochemical route such as various metals, metal oxides, metal sulfides, metal selenides, alloys, bimetallic, etc. In 2007 review, Baranchikov et al. focus on the synthesis of diverse inorganic nanomaterials by application of sonochemical technique [11].

In this chapter, the ultrasound-assisted method as a most successful synthetic tool for the synthesis of nanosize material has been discussed that gives a primary understanding of their fundamental principles and to demonstrate application in the preparation of nanostructured materials. In addition to sonochemistry, the use of ultrasound for ultrasonic spray pyrolysis (USP) has also been discussed.

What Is Sonochemistry?

Chemistry associates with the relations between matter and energy. Sometimes the chemical reaction needed driving force to proceed that is in the form of energy such as heat, radiation, light, electric potential, etc. [12].

In the case of nanostructured material synthesis, the control over chemical reactions is an important aspect, as it affects on morphology of the final product. At present, such control has obtained by manipulating different reaction parameters like time, energy input, and pressure. All types of energies have their own characteristic reaction conditions that are obtained by their typical reaction parameters. In this regard, ultrasonic irradiation offers unusual reaction conditions that cannot be realized by other traditional energy source methods.

Robert Williams Wood was the first to report the influence of sonic waves traveling through liquids. At a molecular or atomic level, the interaction between acoustic waves and matter was not observed. Thus, interaction between the chemical species and ultrasound has absent at molecular level. Rather, acoustic cavitation accounts for the chemical effects (i.e., the generation, growth followed by implosive collapse of bubbles) [13]. In the process of cavitation, generated bubble collapse producing intense heat with high pressures in short time period, which drives high-energy chemical reactions [14]. In detail, acoustic waves (alternating expansive and compressive) by ultrasonic irradiation of liquid produce bubbles (cavities) and make them oscillate. These bubbles store ultrasonic energy very efficiently during their growth. A bubble can overgrow and subsequently collapse, releasing stored ultrasonic energy within short time period (heating and cooling rate of $>10^{10}$ K s^{-1}). This cavitational subsidence is extremely restricted and transient with a pressure of 1,000 bar and a temperature of 5,000 K [15]. The above conditions obtained during acoustic cavitation may result to raise light emission known as sonoluminescence, which was first observed by Frenzel and Schultes during the ultrasonic irradiation of water [16].

Different types of sonochemical apparatus are used for the production of ultrasonic waves like ultrasonic horns, ultrasonic cleaning baths, and flow reactors. For most of the applications, intensity of ultrasonic baths is inadequate, but is however suitable for liquid–solid reactions. In typical laboratory-scale reactions, high-intensity ultrasonic titanium horn with piezoelectric transducer is preferred (Fig. 2). The process of cavitation occurs over a wide array of frequencies (10 Hz–10 MHz).

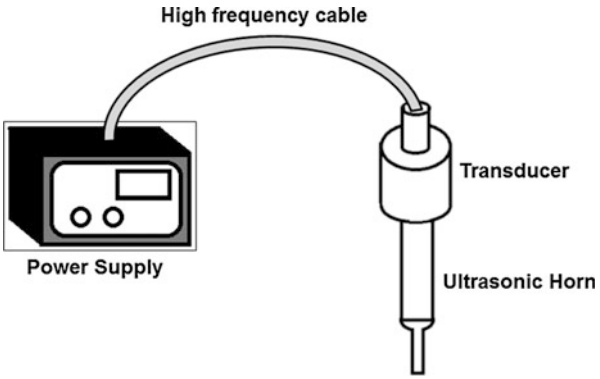

Fig. 2 Schematic representation of ultrasonic horn

Ultrasound-Assisted Nanostructured Material Synthesis

The technique of sonochemistry has shown wide applications for the preparation of various inorganic materials. The core focus is on the preparation of nanosize material. Till date several processes had shown its application for the synthesis of various inorganic materials. In this regard, Suslick and co-workers have a good contribution for the synthesis of a variety of nanostructured metals, alloys, and carbides [17, 18]. Considering widespread applications to make systematic study and understanding of the said method, the chapter has been categorized into materials like metal nanoparticles, metal oxide nanoparticles, and so on (Table 2).

Metal Nanoparticles Synthesis by Sonochemical Rout

Metal nanoparticles offer the latest research on the preparation, characterization, and application of nanoparticles. The structural, optical, electronic, and electrochemical properties of metal nanoparticles are the focus of current research activities. In addition, metal nanoparticles have shown application in cancer treatment, organic reactions, DNA detection, etc. Considering such a wide scope, different research groups synthesize metal nanoparticles by using sonochemical route; for example, Liu et al. reported synthesis of metal nanoparticles having excellent fluorescent properties. The study deals with the use of rapid sonochemical route for the preparation of water-soluble gold nanoclusters (AuNCs) and Au@AgNCs. The AuNCs were synthesized from $HAuCl_4$ by one-step sonochemical route. The morphology of nanomaterial was obtained by HRTEM. The average size of AuNCs was about 1.8 nm with high crystallinity and monodispersity. This is a one-step synthesis of Au@AgNCs by using sonochemical method. The replacement of $HAuCl_4$ by $AgNO_3$ results in the enhancement of the size of the Au@AgNCs [19].

Dhas et al. reported palladium nanoclusters preparation using $Pd(CH_3CO_2)_2$ as a metal precursor and myristyltrimethylammonium bromide as a reductant [$CH_3(CH_2)$

Table 2 Nanomaterials synthesized using ultrasound

Types of nanoparticles	Nanomaterial	Size of nanomaterial	References
Metal nanoparticles	AuNCs and	1.8 nm	[19]
	Au@AgNCs	2.4 nm	
	Palladium	Less than 100	[20]
	Copper and CuOnano	50–70 nm	[21]
	Pd in argon atmosphere	3.6 ± 0.7 nm	[22]
	Pd in nitrogen atmosphere	2.0 ± 0.3 nm	
	Palladium	Less than 10 nm	[23]
	Ruthenium	10–20	[24]
	Fe nanoparticles	3 nm	[25]
	Fe nanoparticles	3–8 nm	[26]
	Gold nano	~40 nm (individual 3 nm)	[27]
	Selenium nanowires	40 ± 7 nm	[32]
Metal sulfides	CdS	10–20 nm	[34]
	Hexagonal CdS	40 nm	[35]
Metal selenides and tellurides	Hollow spherical CdSe	120 nm (individual 5 nm)	[38]
	CdSe	Cluster size 30–40 nm having 7–10 nm crystal size	[35]
	HgSe	30–40 nm in ethylenediamine	[39]
		18–25 ammonia	
	Ag_2Se, CuSe, and PbSe	~70 nm, 30–150 nm and ~160 nm, respectively	[40]
	ZnSe	3–5 nm	[41]
Metal carbides and sulfides	Palladium carbide	Less than 100 nm	[42]
	Molybdenum carbide	2 nm	[43]
Bimetallic nanoparticles/ metal alloys/ metal composites	Composed of gold and palladium	8 nm	[44]
	Fe and Co	Amorphous ferromagnetic less than 100 nm	[45]
	$Co_{20}Ni_{80}$ and $Co_{50}Ni_{50}$	10 nm	[46]
	Fe/Co alloy	~40 nm	[47]
	Pt-Ru	5 and 10 nm	[48]
Metal oxides	Fe_3O_4@SiO_2	4–8 nm	[49]
	SnO_2	3–5 nm	[50]
	Fe_2O_3	100–200 nm diameter pore size of 3–5 nm	[51]
	TiO_2	Less than 10 nm	[52]
	Rare earth metal (Y, Ce, La, Sm, Er) oxides	Fe (3.8 nm); Cr (2.9 nm), Y (3.4 nm), La (4.3 nm), Ce(4.5 nm), Sm(4.2 nm), Er(3.8 nm)	[53]
	MnO_2	10 nm	[54]
	Zinc oxide	39 nm	[55]
	Zinc oxide		[56]

(*continued*)

Table 2 (continued)

Types of nanoparticles	Nanomaterial	Size of nanomaterial	References
		ZnO nanorods, nanocups, nanodisks, nanoflowers, and nanospheres	
	CuO, ZnO, and Co_3O	CuO, ZnO, Co_3O_4, and Fe_3O_4 are 20 nm (length (L)) and 2 nm (width (W)), 340 nm (250), 30 nm, and 20 nm respectively	[57]
Ultrasonic spray pyrolysis (USP)	Titania and ball-in-ball silica–titania composite decorated with Co oxide nanoparticles	Spherical shell	[64]
	Nanostructured carbons	Spherical ball	[65]

13 $N(CH_3)_3Br]$ (NR_4X), in THF or methanol by sonochemical reduction technique at room temperature. Apart from stabilizing effect, NR_4X acts as a reducing agent. The obtained nanocluster shows catalytic property toward carbon-carbon coupling reaction, giving moderate extent of conversions without phosphine ligands [20].

As a follow-up to this work, the author reported sonochemical reduction of copper (II) hydrazine carboxylate $[Cu(N_2H_3COO)_2.2H_2O]$ for the preparation of nanometallic copper clusters in an aqueous medium. The processes of reduction take place under an inert condition for a period of 2–3 h. The powder X-ray diffraction (XRD), FT-IR, and UV-visible studies used to check the ionic copper reduction. The powder XRD analysis of the product shows the formation of a mixture of metallic copper and copper oxide (Cu_2O). Along with the synthesis of copper nanoparticles, the Cu_2O formation can be ascribed to the partial oxidation of copper by in situ generated H_2O_2. However, use of Ar/H_2 (95:5) mixture yields pure metallic copper nanoparticles that could be due to the scavenging action of OH* radicals formed during ultrasonic irradiation. The transmission electron microscopy (TEM) study shows the irregular networking of small particles having porous aggregates in size range of 50–70 nm. The synthesized nanoparticles are found catalytically active toward an "Ullmann reaction" for the aryl halides condensation [21].

Fujimoto et al. has reported synthesis of Pd and Pt nanoparticles by H_2PtCl_6 or K_2PdCl_4 precursors using sonochemical reduction method. In addition to the synthesis, study focuses on atmospheric gas effect on the particle size distribution. They used sonication reactor as shown in Fig. 3. The particle size of Pd was found to be 3.6 ± 0.7 nm under Ar (Pd/Ar) and 2.0 ± 0.3 nm in (Pd/N_2) (Fig. 4). In the case of Pt, a smaller and sharper distribution of the particle size was observed under a Xe atm. This relation has been explained in terms of a hotspot temperature formed by acoustic cavitation [22].

In 2006 Nemamcha et al. reported palladium nanoparticles synthesis using ultrasonic irradiation technique. The stable palladium nanoparticle has been synthesized

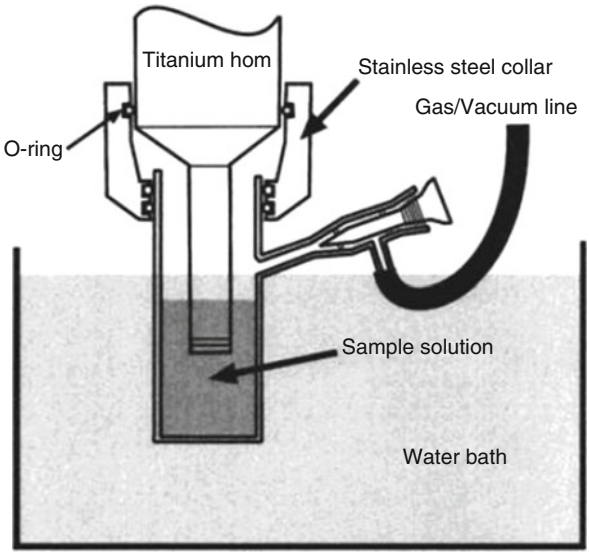

Fig. 3 Schematics of the sonication reactor (Reprinted from Fujimoto et al. [22] with permission from American Chemical Society)

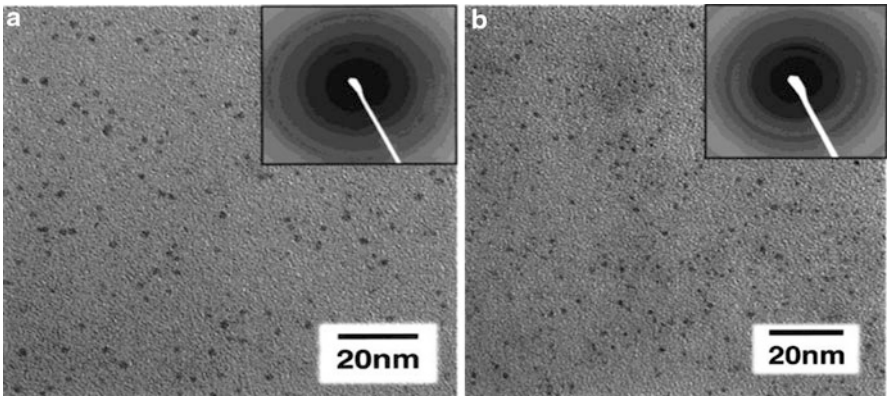

Fig. 4 (**a**, **b**) TEM and SAED pattern of Pd nanoparticles prepared under a N_2 and Xe atmosphere, respectively (Reprinted from Fujimoto et al. [22] with permission from American Chemical Society)

by ultrasonic irradiation of $Pd(NO_3)_2$ solution. Herein, precursor concentration effect on the particle size was studied with different concentrations of palladium (II) nitrate in ethylene glycol and poly (vinylpyrrolidone) (PVP) solutions. The synthesis was done in a glass vessel at 50 kHz ultrasonic waves for 180 min. The pH measurements and UV-visible spectroscopy revealed the reduction of Pd (II) to metallic Pd. The coordination between atomic palladium and carbonyl group of PVP helps for the stabilization of the nanoparticles. The concentration effect of the initial ionic Pd (II) on the morphology of Pd nanoparticle has been examined

by TEM. It has been noticed that the increase of the Pd (II)/PVP molar ratio from 0.13×10^{-3} to 0.53×10^{-3} decreases palladium nanoparticles number with a slight increase in particle size [23]. He et al. applied ultrasound irradiation technique for the preparation of ruthenium nanoparticles. The sonochemical reduction of a ruthenium chloride solution was done by ultrasound frequencies in the range 20–1,056 kHz. The reduction process was checked by UV–vis spectrophotometry. The reduction proceeds sequentially from Ru(III) to Ru(II) to Ru(0) and in almost 13 h. The obtained Ru nanoparticles are in the range of 10–20 nm. In the typical synthesis procedure, 1 mM ruthenium chloride ($RuCl_3$), 0.1 M perchloric acid, 80 mM propanol, and 8 mM sodium dodecyl sulfate (SDS) were used in argon atmosphere under ultrasonic irradiation. The reaction temperature was maintained at 21 ± 2 °C by water circulation through a jacket around the sonication cell. The reaction mass was sonicated at frequencies 213, 357, 647, and 1,056 kHz using different ultrasound transducers. An optimum reduction rate was noticed at the frequency range of 213–355 kHz. The reduction rate of Ru (III) has been observed to be slower, and it may be because of the sequential one-electron reduction steps [24].

In 2004 Khalil et al. reported iron nanoparticles synthesis by ultrasonic irradiation protocol. Synthesis of encapsulated Fe nanoparticles in PEG-400 (FePEG) has been achieved by iron pentacarbonyl and poly (ethylene glycol)-400 (PEG-400) in hexadecane. The prepared material is in the range of 3 nm and is evenly spread in the PEG matrix. Considering the adverse effect of light on ($Fe(CO)_5$), the reaction mixture was sonicated in the dark at 80 % pulsed cycle settings and 100 % intensity. The gas evolution with simultaneous appearance of a black slurry in the reaction vessel indicates $Fe(CO)_5$ decomposition. The decomposited $Fe(CO)_5$ amount was measured by monitoring the gas evolution with respect to time until the achievement of anticipated decomposition [25].

Suslick et al. reported silica-supported Fe nanoparticles by $Fe(CO)_5$ in dry decane solution. The high-intensity ultrasonic probe was used for the irradiation of reaction mixture. After 3 h irradiation at 20 °C under argon, the obtained black powder was filtered and washed with dry pentane. The TEM analysis results showed that the formed iron particles were well dispersed on the SiO_2 surface with 3–8 nm size. To check the catalytic response, the prepared nanoparticles were examined for the Fischer–Tropsch synthesis reaction [26]. Qui et al. reported gold nanoparticles synthesis in the presence of ascorbic acid from potassium dicyanoaurate (I) using sonochemical reduction method. The obtained results reveal the formation of aggregated gold particles with irregular shape in aqueous solution. The study also shows the preparation of needle-shaped gold nanoparticles having mean diameter ~40 nm using polyethylene glycol (PEG-400). The assumed synthesis mechanism of needle-shaped particle formation is because of the chain formation of individual 3 nm gold particles. The formation of gold nanoparticles in the redox reaction attributed to coordination by OH and C-O-C groups of the polymer solvent molecules. Then, these chains aggregate to form needle-shaped particles [27].

Nanowires are likely to play a significant action as active components in the nanoscale electronics and electrochemical, electromechanical, optical, and optoelectronic device fabrication [28–31]. Gates et al. paid a special attention for the

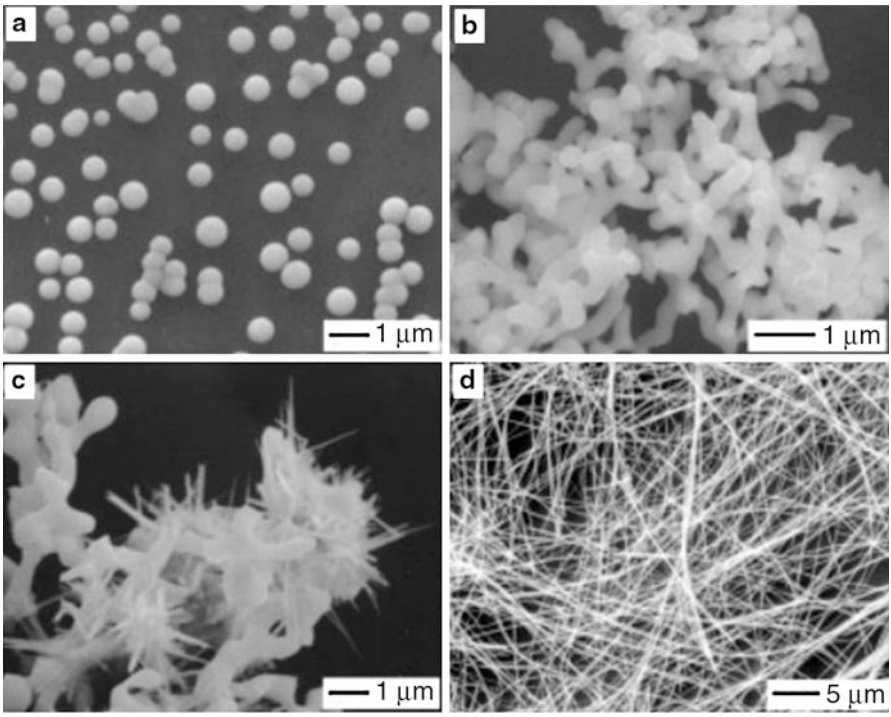

Fig. 5 (**a**–**d**) SEM images dealing with various stages of triangular selenium wire growth (Reprinted from Gates et al. [32] with permission from Wiley-VCH)

preparation of selenium nanowires by cavitational route. The obtained result indicates the formation of nanometer size triangular selenium seeds in alcohol suspension. At room temperature in an aqueous medium, synthesis was carried out by the reduction of selenious acid with hydrazine. The acid reduction results into the formation of amorphous selenium followed by trigonal selenium nanowire formation. The final product obtained consists of nanowires of trigonal selenium with uniform diameter of 40 ± 7 nm (Fig. 5) [32].

Metal Sulfides

Metal sulfides play a vital role because of their wide applications in the diverse fields like laser materials, optical filters, and solar cells [33]. The current research investigation proves that the nanocrystalline metal sulfides show superb performance due to their large volume to mass ratio than that of the bulk. In 2004, Gaoand Wang reported synthesis of cadmium sulfide (CdS) using sonochemical route. The report deals with the CdS nanoparticles deposition on the SnO_2 surface. In a typical synthesis protocol, SnO_2 nanobelts were used as a support. In distilled water,

cadmium chloride and thiourea were added as a metal and sulfur source, respectively. Using horn sonicator, high-intensity ultrasonic frequency of 100 W was used to irradiate reaction mixture for different time intervals of 1–3 h. To expel dissolved oxygen from the reaction mixture, argon gas was bubbled prior to the sonication. The TEM result indicates the formation of nanoparticles in the range of 10–20 nm with nearly spherical shape [34].

Li et al. reported synthesis of hexagonal CdS nanoparticles from $Cd(CH_3CO)_2$ and elemental S as precursors. The nanoparticle formation was done under H_2/Ar (5/95, V/V) atmosphere using ultrasound irradiation. The obtained product contains nanoclusters with an average size of about 40 nm. The control experiments were carried out to investigate the mechanism where hydrogen was acting as a reducing agent, whereas the extreme high temperature brought by the collapse of the bubble accelerates the reduction of elemental S [35].

Metal Selenides and Tellurides

Metal selenides show wide applications in thermoelectric cooling materials, optical filters, optical recording materials, solar cells, supersonic materials, and sensor and laser materials [36, 37]. The nanocrystalline CdSe has been found to be a very useful photoconducting semiconductor material. Zhu et al. reported nanosize CdSe synthesis via sonochemical route with proper mechanism (Fig. 6). This report shows the preparation of hollow spherical CdSe. For fabrication of CdSe hollow spherical assemblies, the ultrasonic waves play an important role. The TEM analysis result shows uniform and regular hollow spheres with 120 nm average diameter. These hollow spheres are the combination of spherical nanoparticles having the diameter of 5 nm (Fig. 7) [38].

Li et al. reported nanosize hexagonal CdSe synthesis by ultrasonic irradiation of $Cd(Ac)_2$ and elemental Se in an H_2/Ar (5/95, V/V) atmosphere. The observed products consist of aggregated nanoclusters with sizes in the range 30–40 nm having 7–10 nm crystal size. The control experiments govern that the hydrogen is acting as a reducing agent and the extreme high temperature developed by the bubble collapse accelerates the reduction of Se [35].

Mercury selenide having electrical properties possessing widespread applications in optoelectronic technology comprises photoconductive, photovoltaic, IR detector, IR emitter, tunable lasers, and thermoelectric coolers. In 2002, Wang et al. reported ultrasonic irradiation protocol for the preparation of mercury selenide from mercury acetate using sodium selenosulfate at room temperature in aqueous reaction medium. The control over particle size was achieved by screening variety of complexing agents. The results showed that the HgSe nanoparticles having different sizes could be obtained by the use of complexing agent like ethylenediamine (EDA), ammonia triethanolamine (TEA), etc. TEA has shown effective control over the size of HgSe particle than that of other complexing agents. The experimental evidence indicates the high TEA concentrations lead to the formation of small particles [39].

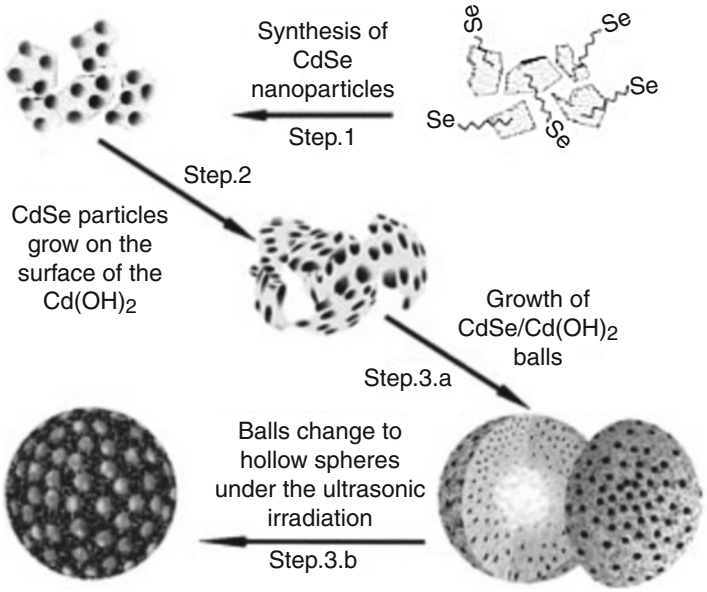

Fig. 6 Proposed mechanism for synthesis of hollow CdSe spheres (Reprinted from Zhu et al. [38] with permission from Wiley-VCH)

Li et al. reported preparation of Ag_2Se, CuSe, and PbSe using ultrasonic irradiation of $AgNO_3$, CuI, and $PbCl_2$, respectively. The metal precursor with selenium in ethylenediamine has been used for the anticipated nanoparticles synthesis. The above reaction mass was irradiated at 18 kHz ultrasonic frequency for 10 h at room temperature. The synthesis was carried out using ultrasonic bath as an ultrasound generator. The synthesis was carried out in a 50 ml stoppered conical flask that was partially submerged in water in a commercial ultrasonic cleaner (Model-H66025, 220 V, 250 W) at room temperature. TEM image shows prepared Ag_2Se nanoparticles are of ~70 nm size, CuSe is in the range of 30–150 nm, and PbSe is of ~160 nm [40].

Zhu et al. reported preparation of ZnSe nanoparticles. The nanosize material has been synthesized by the sonochemical irradiation of selenourea and zinc acetate in an aqueous medium. The reaction mixture was irradiated for 1 h at room temperature under argon atmosphere. The obtained nanomaterial has shown an average size of 3 nm. The time effect on particle size has been studied, and it has been observed that from 1 h to 3 h, the particle size increases from 3 to 5 nm and after 3 h it remains the same at 5 nm [41].

Metal Carbides and Sulfides

Like various inorganic materials, nanosize metal carbides play a vital role in the current research activities such as catalysis. In this regard, Okitsu et al. reported

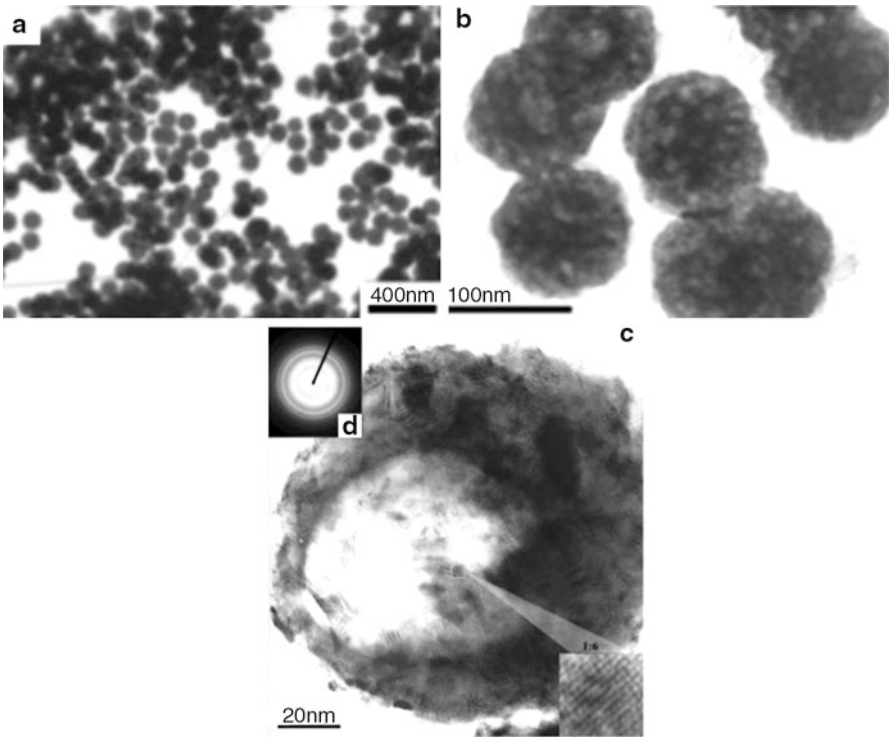

Fig. 7 (**a**, **b**) TEM images of product. (**c**) HRTEM image of individual CdSe with SAED pattern in inset (Reprinted from Zhu et al. [38] with permission from Wiley-VCH)

sonochemical reduction technique for the preparation of palladium nanoparticles with interstitial carbon in aqueous medium. By reduction of tetrachloropalladate (II), metal particles of an interstitial solid solution of palladium carbide were prepared at room temperature. The carbon atom concentration in the Pd particles was controlled by varying the type and the concentration of organic additives. The PdC synthesis is proposed as follows: (1) An active Pd cluster was formed during the formation of palladium particles, (2) organic additives are then adsorbed on the surface of Pd cluster, and (3) finally, carbon atoms diffuse in the metal lattice of Pd. In practice, diverse organic sources are screened, and it has been observed that the increased carbon chain length (methanol < ethanol < hexanol) and the concentration of isopropyl alcohol result in large amount of carbon atoms in the Pd metal [42].

Nanostructured molybdenum carbide was prepared from molybdenum hexacarbonyl slurry in hexadecane. The reaction mixture was sonicated for 3 h at 90 °C under argon environment to yield a black powder. The reason of selecting hexadecane as a solvent is due to its low vapor pressure at the sonication temperature. The obtained powder was filtered inside a dry box followed by several time washing with pentane. TEM showed the formation of 2 nm sized aggregated

particles of the solids. The catalytic activity of the prepared nanomaterial was tested for the cyclohexane dehydrogenation [43].

Bimetallic Nanoparticles/Metal Alloys/Metal Composites

Mizukoshi et al. reported sonochemical technique for bimetallic nanoparticles composed of gold and palladium. Ultrasonic irradiation helps for the reduction of Au (III) and Pd (II) ions from sodium tetrachloroaurate (III) dihydrate and sodium tetrachloropalladate (II), respectively, by (SDS) in an aqueous medium. Along with stabilizing effect, SDS remarkably enhances the reduction rate. A spherical particle with a mean diameter of about 8 nm has been obtained [44].

Amorphous ferromagnetic alloys consisting of Fe and Co have revealed excellent soft magnetic properties superior over conventional materials. Some applications comprise magnetic storage media and power transformers [45]. Considering such application, Shafi et al. reported preparation of nanosize amorphous alloy powders of $Co_{20}Ni_{80}$ and $Co_{50}Ni_{50}$ by sonochemical decomposition technique. The volatile organic precursors, $Co(NO)(CO)_3$ and $Ni(CO)_4$, in decalin were used at 273 K, under an argon pressure of 100–150 kPa. The obtained results by the analytical tools like SEM, TEM, SAED, and XRD reveal the amorphous nature of these particles. TEM result of the $Co_{20}Ni_{80}$ showed uniform particles with sizes less than 10 nm. The obtained material has shown the superparamagnetic characteristics [46].

Nanoparticles of the Fe/Co alloy were synthesized by a mixture of $Fe(CO)_5$ and $Co(NO)(CO)_3$ in diphenylmethane (DPhM) solution under argon atmosphere using ultrasonic irradiation method. The obtained product is an amorphous material with 10 nm diameter size. By annealing in argon atmosphere at 600 °C for 5 h, an air-stable Fe/Co alloy is obtained with ~40 nm particle size. The nanoparticles consist of a metal alloy core and a coated shell. The prepared nanoparticles demonstrate an excellent storage stability and magnetic performance [47].

Pt-Ru bimetallic system has great interest because of catalytic application for methanol oxidation in direct methanol fuel cells. In 2006, Vinodgopal et al. reported synthesis of colloidal Pt-Ru bimetallic nanoparticles by aqueous phase sonochemical reduction of Pt(II) and Ru(III). The synthesis was performed at the frequency of 213 kHz and at temperature of 20 °C. The circulating water through a jacket around the sonication cell helps to retain constant temperature during the sonication. However, TEM result specifies the sequential reduction of the Pt(II) followed by the Ru (III) giving core shell (Pt@Ru) morphology. Application of SDS, as a stabilizer, helps for the formation of particles in the range of 5 and 10 nm. PVP enhances the rate of reduction giving ultrasmall bimetallic particles of up to 5 nm [48].

Metal Oxide Nanoparticles

Metal oxides show a crucial role in the field of physics, chemistry, and materials science. The elements form a diverse range of oxide compounds having a large

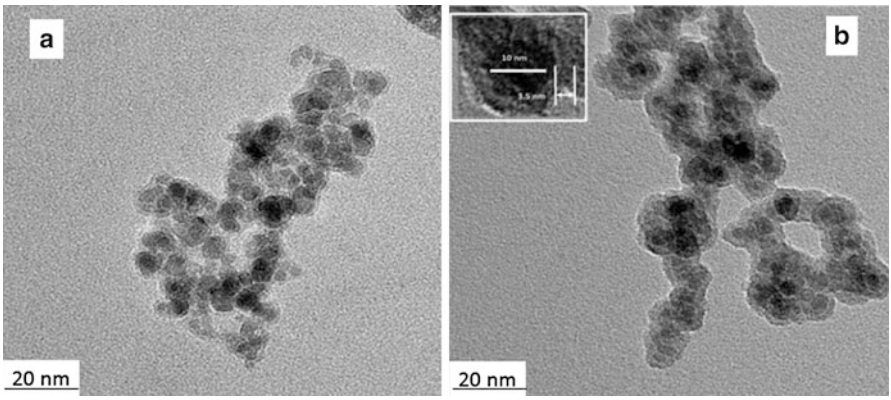

Fig. 8 TEM images of Fe_3O_4@SiO_2NPs after 1 h (**a**) and 3 h (**b**) of sonication. Zoomed image of a single core shell particle is shown in the inset of *panel b* (Reprinted from Morel et al. [49] with permission from American Chemical Society)

number of structural geometries. In technological fields, metal oxides have application for the fabrication of various electronic gadgets such as piezoelectric devices, microelectronic circuits, sensors, and fuel cells. In addition, it proves application in coatings (passivation of surfaces against corrosion) and in catalysis. Nanoparticles of metal oxide displayed unique physical and chemical properties because of their restricted size and a high density at corner or edge sites.

Considering their wide applicability, metal oxide nanoparticles have received attention from researchers toward the synthesis of such nanomaterials. Morel et al. reported a rapid synthesis of monodispersed non-aggregated Fe_3O_4@SiO_2 nanoparticles by sonochemical technique (NPs) (Fig. 8). The coprecipitation of Fe (II) and Fe(III) under ultrasonic effect in aqueous solutions gives smaller Fe_3O_4 NPs with a size distribution of 4–8 nm. Sonication helps to control the thickness of the silica shell in the range of several nanometers. At 20 kHz ultrasonic field frequency, silica-coated Fe_3O_4 NPs have been obtained by alkaline hydrolysis of tetraethyl ortho-silicate in ethanol-water mixture. Core shell Fe NPs were synthesized by sonochemical route showing a high magnetization value than that of nanoparticles prepared under silent conditions, which is due to the high speed of sonochemical coating and better control over silica deposition [49].

Srivastava et al. prepared nanosize mesoporous SnO_2 (tin oxide) by a sonochemical method. Synthesis was done by using tin ethoxide precursor and cetyltrimethylammonium bromide as the structure-directing agent. The mesoporous SnO_2 formation was confirmed by comparing its wide-angle X-ray spectra with previously reported data. The pore size measurement by TEM analysis shows particle size in the range of 3–5 nm. The prepared porous SnO_2 was used in dye-sensitized solar cells [50].

In continuation to above work, the same authors reported the preparation of mesoporous iron oxides using iron (III) ethoxide and cetyltrimethylammonium bromide (CTAB) as precursor and organic structure-directing agent, respectively.

The synthesis was done by ultrasonic irradiation followed by calcination and solvent extraction for the removal of surfactant. The XRD, TEM, TGA, and BET surface area measurements of calcined material give detailed idea about the synthesized nanomaterial. The particles of Fe_2O_3 possess irregular shape having 100–200 nm diameter with a pore size of 3–5 nm. The as-prepared amorphous Fe_2O_3 has revealed paramagnetic properties, while it shows good magnetic properties after calcination at 350 °C. The prepared mesoporous Fe_2O_3 shows high conversion with a high selectivity in the oxidation reaction of cyclohexane under mild reaction conditions [51].

Titanium oxide (TiO_2) was used as a photocatalyst for treating environmental contaminants. Yu et al. focused on the mesoporous TiO_2 synthesis. The reaction was carried under high-intensity ultrasound irradiation. The reaction was done in both the conditions as with and without use of copolymer. In the absence of thermal treatment, agglomerates of monodispersed TiO_2 particles are formed. The obtained catalyst exhibited better activities for degradation of n-pentane than that of the commercially available photocatalyst P25. The rate of degradation by mesoporous TiO_2 synthesized using triblock copolymer was about double than that of P25. The high catalytic activities of the TiO_2 with a bicrystalline framework can be endorsed to the combined effect of high surface area and mesopores nature [52].

Wang et al. focused on the synthesis of rare earth metal (Y, Ce, La, Sm, Er) oxides by sonochemical method. The oxide synthesis was obtained by the use of SDS as the surfactant, urea as the precipitating agent, and the nitrate salts of metals as the precursors of metal ions, except $ZrO(NO_3)_2$ precursor for zirconium. The molar ratio of metal ion/SDS/urea was 1/2/30, respectively. The reaction mixture was sonicated for 3 h by a high-intensity ultrasonic probe (Misonix, XL sonifier, 1.13 cm diameter Ti horn, 20 kHz, 100 W/cm^2) for the preparation of metal oxides. After sonication, the suspension was centrifuged, washed, and dried, which gives the desired material [53].

Zhu et al. reported synthesis of MnO_2 nanoparticles confined in ordered mesoporous carbon using ultrasound irradiation technique. The MnO_2 nanoparticles are synthesized in the pore channels of ordered mesoporous carbon CMK3. The TEM result shows obtained nanoparticles are in the range of 10 nm [54].

Bhatte et al. reported additives free nanocrystalline zinc oxide synthesis using zinc acetate and 1,4-butanediol. For the desired product, formation reaction was performed under ultrasonic waves. Ultrasonic horn was used as a source of sonic waves. The use of 1,4-butanediol gives double merits in the form of solvent and capping agent that eliminates addition of excess additives [55].

However Jung et al. reported shape-selective ZnO nanoparticles using sonochemical synthesis route. The core focus of this study allied with the shape-selective ZnO nanostructure preparation. The idea comprised synthesis of nanomaterials such as nanorods, nanocups, nanodisks, nanoflowers, and nanospheres (Fig. 9). The precursor concentration, type of hydroxide anion-producing agents, sonication time, and the type of capping agent are key factors in the shape-selective ZnO nanomaterial synthesis. Zinc nitrate hexahydrate ($Zn(NO_3)_2 \cdot 6H_2O$) and hexamethylenetetramine (HMT, $(CH_2)_6\ N_4$) were used for the synthesis.

The preparation of nanomaterial was achieved under ambient reaction conditions using sonochemical apparatus of 20 kHz frequency. In order to prepare ZnO nanorods,

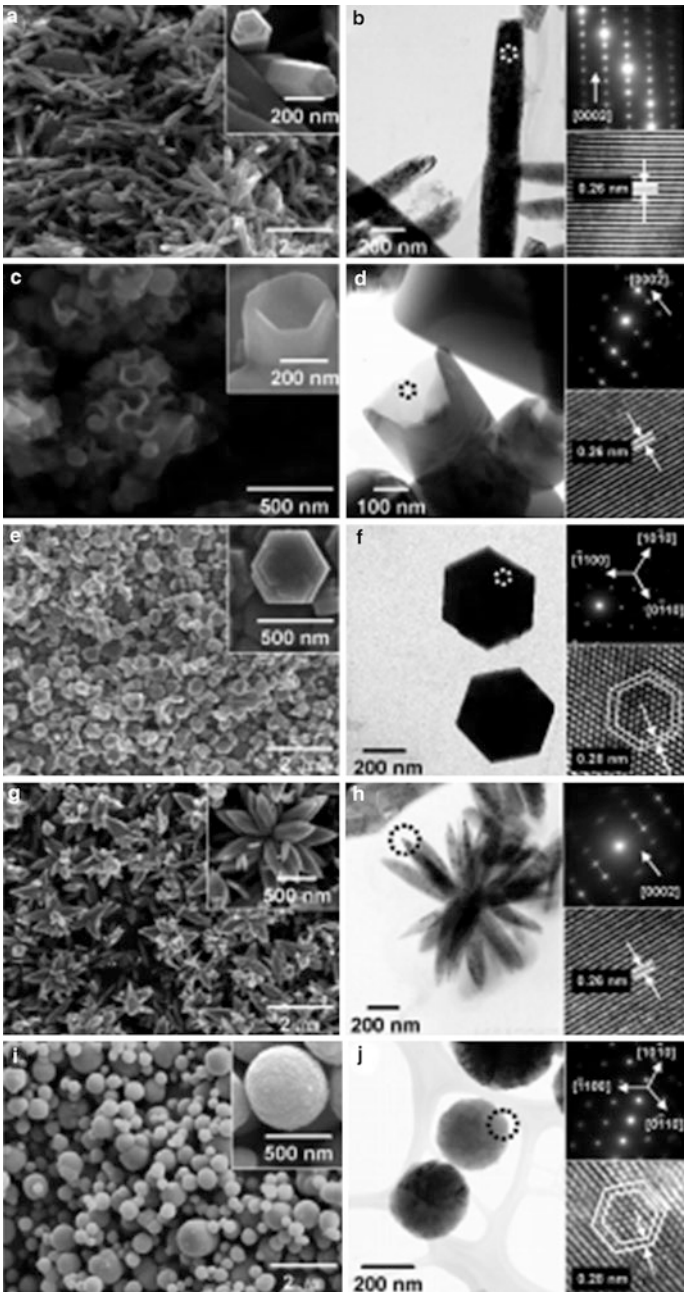

Fig. 9 SEM (*left*) and TEM (*right*) images of ZnO nanostructures. (**a**, **b**) Nanorods. (**c**, **d**) Nanocups. (**e**, **f**) Nanodisks. (**g**, **h**) Nanoflowers. (**i**, **j**) Nanospheres. A corresponding electron diffraction pattern and a HRTEM image were inserted as an upper and a lower inset in TEM images, respectively (Reprinted from Jung et al. [56] with permission from American Chemical Society)

a 50 W ultrasonic wave power (intensity of 39.5 W/cm^2) was introduced for 30 min. For ZnO nanocups synthesis, a mixture of 50 mL 0.2 M $Zn(NO_3)_2 \cdot 6H_2O$ solution and 50 mL 0.2 M HMT solution was sonicated for 2 h with 39.5 W/cm^2 intensity. However, ZnO nanodisk preparation was achieved by triethyl citrate, wherein 100 mL aqueous solution containing 0.01 M $Zn(NO_3)_2 \cdot 6H_2O$, 0.01 M HMT, and 0.1 M triethyl citrate was sonicated for 30 min with 39.5 W/cm^2 intensity. In addition to this, $Zn(CH_3COO)_2 \cdot 2H_2O$ as zinc cation precursors and ammonia–water (28–30 wt%,) combination as hydroxide anion supplier were used for the synthesis of ZnO nanoflowers and nanospheres. For ZnO nanoflowers, preparation mixture of 0.01 M zinc acetate dihydrate and 1.57 M ammonia concentrations was reported. However, ZnO nanosphere synthesis was achieved by addition of triethyl citrate in the mixture of 90 mL zinc acetate dihydrate and 10 mL ammonia–water solution. The reaction mixture was irradiated at an intensity of 39.5 W/cm^2 for 30 min [56].

Vijaya Kumar et al. reported transition metal oxide nanoparticles like CuO, ZnO, and Co_3O from metal acetates using sonochemical route. Solvent effect (water and 10 % water-N,N dimethylformamide (DMF)) on particle sizes, morphology, and yields of the products was investigated [57].

Ultrasonic Spray Pyrolysis (USP)

In sonochemistry, ultrasound directly induces chemical reaction; however, in USP, ultrasound is not directly employed in chemical reactions. In USP, ultrasound is to offer the phase separation of one micro-droplet reactor from another. The concept of sonochemistry is associated to a low frequency with high-intensity ultrasound (typically 20 kHz), whereas USP usually utilize a high frequency with low-intensity ultrasound (e.g., 2 MHz). This technique utilizes ultrasound for nebulizing precursor solutions that help to produce the micron-sized droplets. The prepared droplets will work as individual micron-sized chemical reactors. The produced droplets by ultrasonic nebulization are heated in a gas flow and then subjected to chemical reaction.

Technique proves wide applications in industry for the preparation of ultrafine particle and nanoparticle. In addition, it has applications for film deposition. Since it required simple and continuous setup, it can be applied simply for mass production. Overall, technique involves generation of aerosols by nebulizer followed by the thermal decomposition [58].

In accordance with traditional techniques, USP has several advantages like continuous operation technique, easy control, and high product purity. Methods work excellent for the synthesis of spherical particle [59, 60]. USP is a continuous flow process work in both small-scale and large-scale productions with superb reproducibility. In addition, USP showed main applications toward preparation of composite materials. In 1927, Wood and Loomis reported the process of droplet formation by low-frequency ultrasound application [61]. In 1962, Lang has experimentally shown the effect of ultrasonic frequency and droplet size [62].

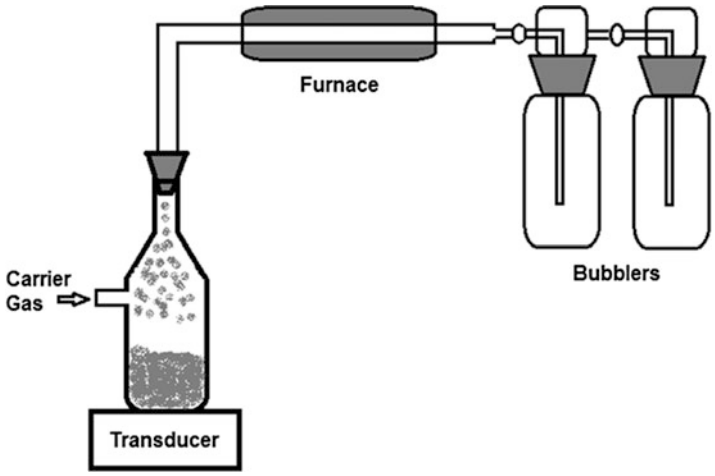

Fig. 10 Schematic illustration of typical USP apparatus

In USP, the first step, that is, the formation of liquid droplets, was achieved by capillary waves from ultrasonic nebulization [63]. The prepared droplets were then carried into a heated zone by carrier gases like Ar, O_2, and N_2. The next step is solvent evaporation from the droplet surface where the droplets quickly shrink, and further heat supply results in supersaturation; this is the point where solute gets precipitates on the surface of droplet. The decomposition may prepare intermediate in the form of porous or hollow particles, which may form solid particles due to densification. A typical USP apparatus consists of a vessel having transducer at the base fitted with a mist carrying gas stream to the tubular furnace; collected chambers are located at the furnace exit (Fig. 10). On close inspection, using USP method, cobalt nanoparticles embedded on the silica nanoparticles resulting in spherical porous material can be observed (Fig. 11).

Suslick and co-workers reported titania nanomaterials using the USP synthesis protocol. The synthesis consists of different morphological forms like porous, hollow, and ball in ball. Aqueous solution consists of a mixture of silica nanoparticles and titanium complex; when subjected for USP process, it gives titania/silica nanocomposites (Fig. 12a). After selective etching of the silica by HF, it produces a porous titania microsphere (Fig. 12b). Initial etching gives a ball-in-ball structure comprising silica core that is covered with porous titania shell outside (Fig. 12c, d). However, full etching results in the disappearance of core giving only porous spherical shells of titania [64].

The USP technique shows application for the formation of porous carbon. In this regard, Skrabalak and Suslick applied this technique for the preparation of several carbon nanostructures by alkali halocarboxylate decomposition (Fig. 13). When compared to tedious multistep traditional processes for porous carbon synthesis, this new one-step process approach eliminates expensive template materials. Depending on the type of alkali halocarboxylates, a diverse range of nanostructures have been prepared [65].

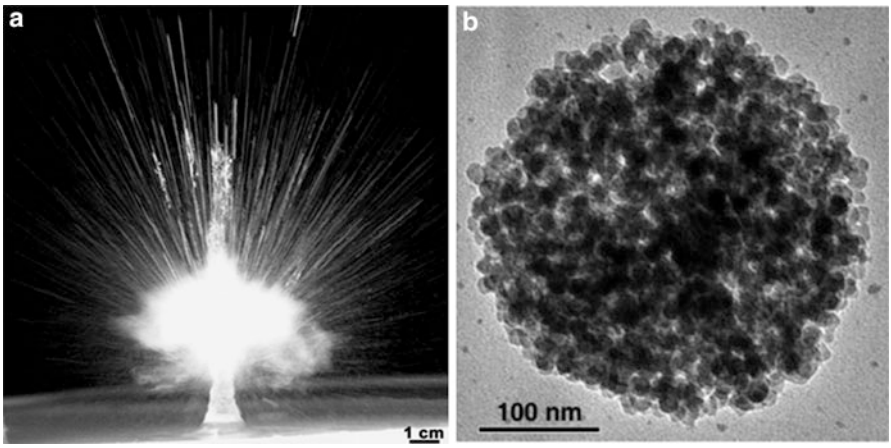

Fig. 11 (**a**) Macrophotograph of an ultrasonic fountain and mist. (**b**) TEM image of cobalt-doped porous silica nanosphere (Reprinted from Suh and Suslick [63] with permission from American Chemical Society)

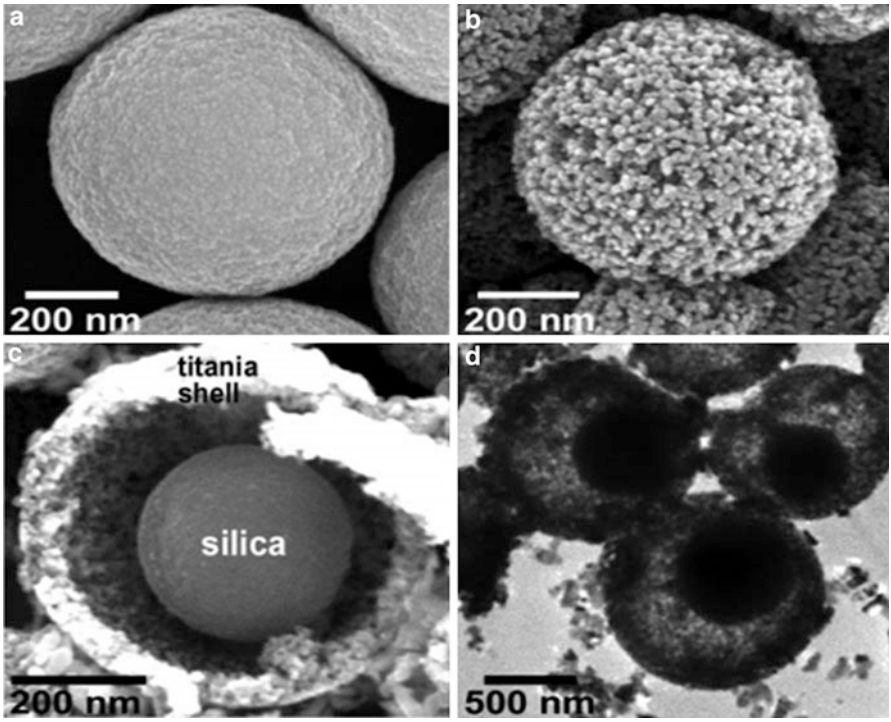

Fig. 12 Electron micrographs of (**a**) silica–titania composite; (**b**) porous titania obtained by HF treatment; (**c**) SEM and (**d**) TEM image of ball-in-ball silica–titania composite decorated with Co oxide nanoparticles after partial etching with HF (Reprinted from Suh et al. [64] with permission from Wiley-VCH)

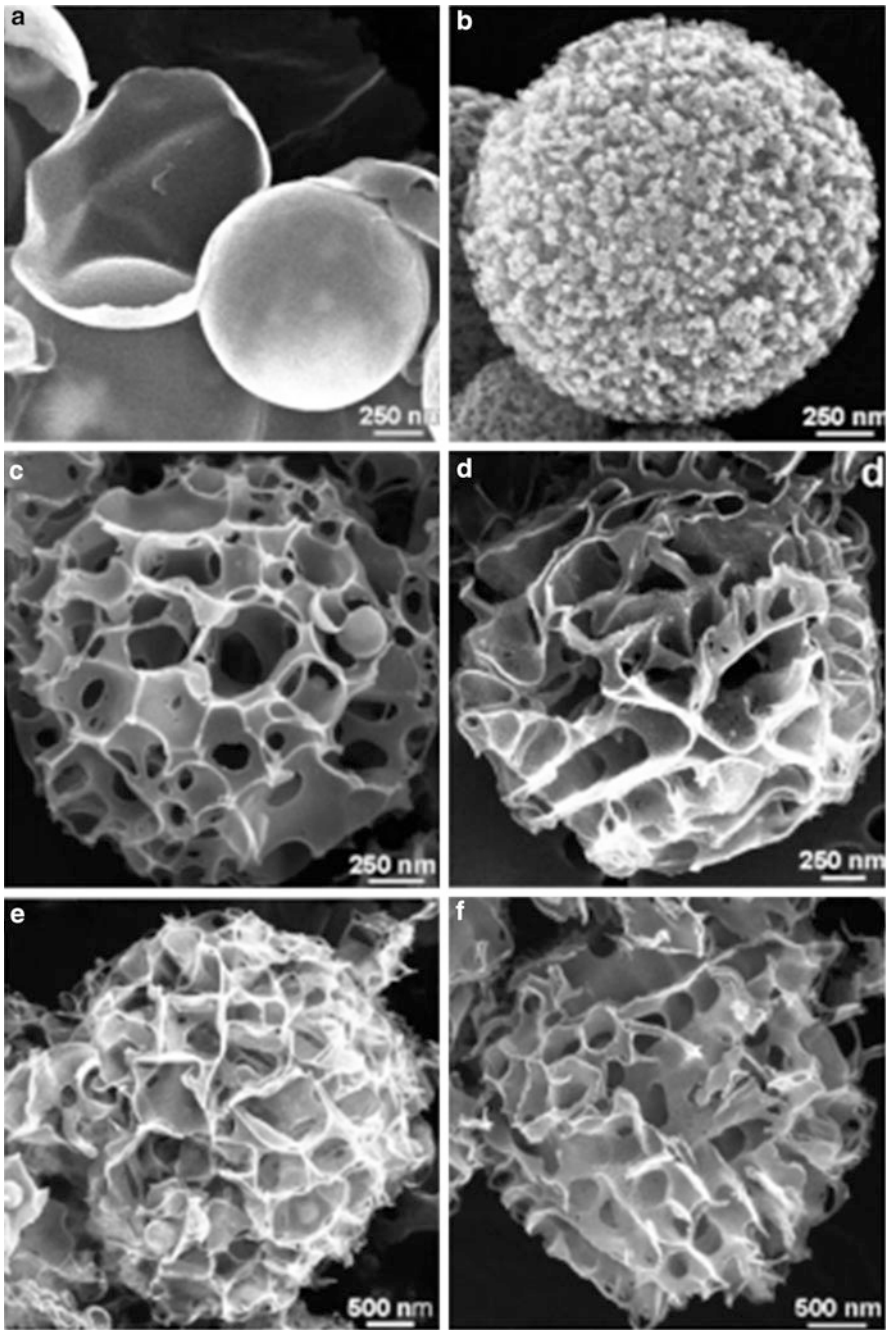

Fig. 13 SEM images of USP porous carbons from various precursors: (**a**) lithium chloroacetate, (**b**) lithium dichloroacetate, and (**c**) sodium chloroacetate, (**d**) sodium dichloroacetate, (**e**) potassium chloroacetate, and (**f**) potassium dichloroacetate (Reprinted from Skrabalak and Suslick [65] with permission from American Chemical Society)

Conclusion

In summary, this chapter focused on the use of ultrasound as an energy source by sonochemical technique or USP method. Along with the basic mechanism of sonochemistry, the chapter covers application of sonochemistry and USP for the synthesis of nanosize materials. Representative examples from different classes of inorganic materials like metal, metal oxide, sulfides, selenides, carbides, alloys, etc., have been discussed.

References

1. A. Roucoux, J. Schulz, H. Patin, Reduced transition metal colloids: a novel family of reusable catalysts? Chem. Rev. **102**, 3757–3778 (2002)
2. T. Hyeon, M. Fang, K.S. Suslick, Nanostructured molybdenum carbide: sonochemical synthesis and catalytic properties. J. Am. Chem. Soc. **118**, 5492–5493 (1996)
3. K. Bhatte, P. Tambade, S. Fujita, M. Arai, B. Bhanage, Microwave-assisted additive free synthesis of nanocrystalline zinc oxide. Powder Technol. **203**, 415–418 (2010)
4. K. Bhatte, D. Sawant, R. Watile, B. Bhanage, A rapid, one step microwave assisted synthesis of nanosize zinc oxide. Mater. Lett. **69**, 66–68 (2012)
5. K. Bhatte, D. Sawant, K. Deshmukh, B.M. Bhanage, Additive free microwave assisted synthesis of nanocrystalline $Mg(OH)_2$ and MgO. Particuology **10**, 384–387 (2012)
6. M. Bhosale, K. Bhatte, B.M. Bhanage, A rapid, one pot microwave assisted synthesis of nanosize cuprous oxide. Powder Technol. **235**, 516–519 (2013)
7. K.M. Deshmukh, Z.S. Qureshi, K.D. Bhatte, K.A. Venkatesan, T.G. Srinivasan, P.R. Vasudeva Rao, B.M. Bhanage, One-pot electrochemical synthesis of palladium nanoparticles and their application in the Suzuki reaction. New J. Chem. **35**, 2747–2751 (2011)
8. A. Patil, S. Lanke, K. Deshmukh, A. Pandit, B. Bhanage, Solar energy assisted palladium nanoparticles synthesis in aqueous medium. Mater. Lett. **79**, 1–3 (2012)
9. A. Patil, D. Patil, B. Bhanage, ZnO nanoparticle by solar energy and their catalytic application for α-amino phosphonates synthesis. Mater. Lett. **86**, 50–53 (2012)
10. A. Patil, D. Patil, B. Bhanage, Selective and efficient synthesis of decahedral palladium nanoparticles and its catalytic performance for Suzuki coupling reaction. J. Mol. Catal. A **365**, 146–153 (2012)
11. A.Y. Baranchikov, V.K. Ivanov, Y.D. Tretyakov, Sonochemical synthesis of inorganic materials. Russ. Chem. Rev. **76**, 133–151 (2007)
12. K.S. Suslick, *Ultrasound: Its Chemical, Physical, and Biological Effects* (Wiley-VCH, New York, 1988)
13. K.S. Suslick, S.J. Doktycz, The effects of ultrasound on solids. Adv. Sonochem. **1**, 197–230 (1990)
14. E.B. Flint, K.S. Suslick, The temperature of cavitation. Science **253**, 1397–1399 (1991)
15. S.J. Doktycz, K.S. Suslick, Interparticle collisions driven by ultrasound. Science **247**, 1067–1069 (1990)
16. H. Frenzel, H. Schultes, Luminescenz im ultraschallbeschickten wasser (Luminescence in the ultrasound-fed water). Z. Phys. Chem. **27b**, 421–424 (1934)
17. J.H. Bang, K.S. Suslick, Applications of ultrasound to the synthesis of nanostructured materials. Adv. Mater. **22**, 1039–1059 (2010)
18. K.S. Suslick, S.B. Choe, A.A. Cichowlas, M.W. Grinstaff, Sonochemical synthesis of amorphous iron. Nature **353**, 414–416 (1991)
19. H. Liu, X. Zhang, X. Wu, L. Jiang, C. Burda, J.-J. Zhu, Rapid sonochemical synthesis of highly luminescent non-toxic AuNCs and Au@AgNCs and Cu (II) sensing. Chem. Commun. **47**, 4237–4239 (2011)

20. N.A. Dhas, A. Gedanken, Sonochemical preparation and properties of nanostructured palladium metallic clusters. J. Mater. Chem. **8**, 445–450 (1998)
21. N.A. Dhas, C. Paul Raj, A. Gedanken, Synthesis, characterization, and properties of metallic copper nanoparticles. Chem. Mater. **10**, 1446–1452 (1998)
22. T. Fujimoto, S. Terauchi, H. Umehara, I. Kojima, W. Henderson, Sonochemicalpreparation of single-dispersion metal nanoparticles from metal salts. Chem. Mater. **13**, 1057–1060 (2001)
23. A. Nemamcha, J.-L. Rehspringer, D. Khatmi, Synthesis of palladium nanoparticles by sonochemicalreduction of palladium(II) nitrate in aqueous solution. J. Phys. Chem. B **110**, 383–387 (2006)
24. Y. He, K. Vinodgopal, M. Ashokkumar, F. Grieser, Sonochemical synthesis of ruthenium nanoparticles. Res. Chem. Intermed. **32**, 709–715 (2006)
25. H. Khalil, D. Mahajan, M. Rafailovich, M. Gelfer, K. Pandya, Synthesis of zerovalent-nanophase metal particles stabilized with poly(ethylene glycol). Langmuir **20**, 6896–6903 (2004)
26. K.S. Suslick, T. Hyeon, M. Fang, A.A. Cichowlas, Sonochemical synthesis of nanostructured catalysts. Mater. Sci. Eng. **A204**, 186–192 (1995)
27. X.F. Qui, J.J. Zhu, H.Y. Chen, Controllable synthesis of nanocrystalline gold assembled whiskery structures via sonochemical route. J. Cryst. Growth **257**, 378–383 (2003)
28. Z.L. Wang, Characterizing the structure and properties of individual wire-like nanoentities. Adv. Mater. **12**, 1295–1298 (2000)
29. X. Duan, Y. Huang, Y. Cui, J. Wang, C.M. Lieber, Indium phosphide nanowires as building blocks for nanoscale electronic and optoelectronic devices. Nature **409**, 66–69 (2001)
30. C. Dekker, Carbon nanotubes as molecular quantum wires. Phys. Today **May**, 22–28 (1999)
31. S. Frank, P. Poncharal, Z.L. Wang, W.A. de Heer, Carbon nanotube quantum resistors. Science **280**, 1744–1746 (1998)
32. B. Gates, B. Mayers, A. Grossmn, Y. Xia, A sonochemical approach to the synthesis of crystalline selenium nanowires in solutions and on solid supports. Adv. Mater. **14**, 1749–1752 (2002)
33. S.T. Lakshmikvmar, A.C. Rastogi, Selenization of Cu and In thin films for the preparation of selenide photo-absorber layers in solar cells using Se vapour source. Sol. Energy Mater. Sol. Cells **32**, 7–19 (1994)
34. T. Gao, T. Wang, Sonochemical synthesis of SnO_2nanobelt/CdS nanoparticle core/shell heterostructures. Chem. Commun. **22**, 2558–2559 (2004)
35. H.-l. Li, Y.-c. Zhu, S.-g. Chen, O. Palchik, J.-p. Xiong, Y. Koltypin, Y. Gofer, A. Gedanken: A novel ultrasound-assisted approach to the synthesis of CdSe and CdS nanoparticles. J. Solid State Chem. **172,** 102–110 (2003)
36. W.Z. Wang, Y. Geng, P. Yan, F.Y. Liu, Y. Xie, Y.T. Qian, A novel mild route to nanocrystallineselenides at room temperature. J. Am. Chem. Soc. **121**, 4062–4063 (1999)
37. W.Z. Wang, P. Yan, F.Y. Liu, Y. Xie, Y. Geng, Y.T. Qian, Preparation and characterization of nanocrystalline Cu_2–xSe by a novel solvothermal pathway. J. Mater. Chem. **8**, 2321–2322 (1998)
38. J.-J. Zhu, S. Xu, H. Wang, J.-M. Zhu, H.-Y. Chen, Sonochemical synthesis of CdSe hollow spherical assemblies via an in-situ template route. Adv. Mater. **15**, 156–159 (2003)
39. H. Wang, S. Xu, X.-N. Zhao, J.-J. Zhu, X.-Q. Xin, Sonochemical synthesis of size-controlled mercury selenide nanoparticles. Mater. Sci. Eng. B **96**, 60–64 (2002)
40. B. Li, Y. Xie, J. Huang, Y. Qian, Sonochemical synthesis of silver, copper and lead selenides. Ultrason. Sonochem. **6**, 217–220 (1999)
41. J. Zhu, Y. Koltypin, A. Gedanken, General sonochemicalmethod for the preparation of nanophasicselenides: synthesis of ZnSenanoparticles. Chem. Mater. **12**, 73–78 (2000)
42. K. Okitsu, Y. Nagata, Y. Mizukoshi, Y. Maeda, H. Bandow, T.A. Yamamoto, Synthesis of palladium nanoparticles with interstitial carbon by sonochemical reduction of tetrachloro-palladate(II) in aqueous solution. J. Phys. Chem. B **101**, 5470–5472 (1997)
43. K.S. Suslick, T. Hyeon, M. Fang, J.T. Ries, A.A. Cichowlas, Sonochemical synthesis of nanophase metals, alloys, and carbides. Mater. Sci. Forum **225–227**, 903–912 (1996)

44. Y. Mizukoshi, K. Okitsu, Y. Maeda, T.A. Yamamoto, R. Oshima, Y. Nagata, Sonochemical preparation of bimetallic nanoparticles of gold/palladium in aqueous solution. J. Phys. Chem. B **101**, 7033–7037 (1997)
45. T. Egami, Magnetic amorphous alloys: physics and technological applications. Rep. Prog. Phys. **47**, 1601–1725 (1984)
46. K. Shafi, A. Gedanken, R. Prozorov, Sonochemical preparation and characterization of nanosized amorphous Co–Ni alloy powders. J. Mater. Chem. **8**, 769–773 (1998)
47. Q. Li, H. Li, V.G. Pol, I. Bruckental, Y. Koltypin, J. Calderon-Moreno, I. Nowik, A. Gedanken, Sonochemical synthesis, structural and magnetic properties of air-stable Fe/Co alloy nanoparticles. New J. Chem. **27**, 1194–1199 (2003)
48. K. Vinodgopal, Y. He, M. Ashokkumar, F. Grieser, Sonochemically prepared platinum − ruthenium bimetallic nanoparticles. J. Phys. Chem. B **110**, 3849–3852 (2006)
49. A.-L. Morel, S.I. Nikitenko, K. Gionnet, A. Wattiaux, J. Lai-Kee-Him, C. Labrugere, B. Chevalier, G. Deleris, C. Petibois, A. Brisson, M. Simonoff, Sonochemical approach to the synthesis of Fe_3O_4@SiO_2 core − shell nanoparticles with tunable properties. ACS Nano **2**, 847–856 (2008)
50. D.N. Srivastava, S. Chappel, O. Palchik, A. Zaban, A. Gedanken, Sonochemical synthesis of mesoporous tin oxide. Langmuir **18**, 4160–4164 (2002)
51. D.N. Srivastava, N. Perkas, A. Gedanken, I. Felner, Sonochemicalsynthesis of mesoporousiron oxide and accounts of its magnetic and catalytic properties. J. Phys. Chem. B **106**, 1878–1883 (2002)
52. J.C. Yu, L. Zhang, J. Yu, Direct sonochemical preparation and characterization of highly active mesoporous TiO_2 with a bicrystalline framework. Chem. Mater. **14**, 4647–4653 (2002)
53. Y. Wang, L. Yin, A. Gedanken, Sonochemical synthesis of mesoporous transition metal and rare earth oxides. Ultrason. Sonochem. **9**, 285–290 (2002)
54. S. Zhu, H. Zhou, M. Hibino, I. Honma, M. Ichihara, Synthesis of MnO_2 nanoparticles confined in ordered mesoporous carbon using a sonochemical method. Adv. Funct. Mater. **15**, 381–386 (2005)
55. K. Bhatte, S. Fujita, M. Arai, A. Pandit, B. Bhanage, Ultrasound assisted additive free synthesis of nanocrystalline zinc oxide. Ultrason. Sonochem. **18**, 54–58 (2011)
56. S.-H. Jung, E. Oh, K.-H. Lee, Y. Yang, C.G. Park, W. Park, S.-H. Jeong, Sonochemical preparation of shape-selective ZnO nanostructures. Cryst. Growth Des. **8**, 265–269 (2008)
57. R. Vijaya Kumar, Y. Diamant, A. Gedanken, Sonochemical synthesis and characterization of nanometer-size transition metal oxides from metal acetates. Chem. Mater. **12**, 2301–2305 (2000)
58. T.T. Kodas, M. Hampden-Smith, *Aerosol Processing of Materials* (Wiley-VCH, New York, 1999)
59. K. Okuyama, W. Lenggoro, Preparation of nanoparticles via spray route. Chem. Eng. Sci. **58**, 537–547 (2003)
60. G.L. Messing, S.-C. Zhang, G.V. Jayanthi, Ceramic powder synthesis by spray pyrolysis. J. Am. Ceram. Soc. **76**, 2707 (1993)
61. R.W. Wood, A.L. Loomis, The physical and biological effects of high-frequency sound-waves of great intensity. Phil. Mag. **7**, 417–436 (1927)
62. R.J. Lang, Ultrasonic atomization of liquids. J. Acoust. Soc. Am. **34**, 6–8 (1962)
63. W.H. Suh, K.S. Suslick, Magnetic and porous nanospheres from ultrasonic spray pyrolysis. J. Am. Chem. Soc. **127**, 12007–12010 (2005)
64. W.H. Suh, A.R. Jang, Y.-H. Suh, K.S. Suslick, Porous, hollow, and ball-in-ball metal oxide microspheres: preparation, endocytosis, and cytotoxicity. Adv. Mater. **18**, 1832–1837 (2006)
65. S.E. Skrabalak, K.S. Suslick, Porous carbon powders prepared by ultrasonic spray pyrolysis. J. Am. Chem. Soc. **128**, 12642–12643 (2006)